

Evolution of pion HBT radii from RHIC to LHC – Predictions from ideal hydrodynamics

Evan Frodermann, Rupa Chatterjee and Ulrich Heinz

Department of Physics, The Ohio State University, Columbus, OH 43210, USA

Abstract. We present hydrodynamic predictions for the charged pion HBT radii for a range of initial conditions covering those presumably reached in Pb+Pb collisions at the LHC. We study central ($b=0$) and semi-central ($b=7$ fm) collisions and show the expected increase of the HBT radii and their azimuthal oscillations. The predicted trends in the oscillation amplitudes reflect a change of the final source shape from out-of-plane to in-plane deformation as the initial entropy density is increased.

1. Introduction

Ideal fluid dynamics has been used successfully to reproduce many aspects of heavy-ion collisions at RHIC [1]. However, even though the hydrodynamic model correctly describes the hadron spectra at low transverse momenta, it fails to reproduce the transverse HBT radii (R_s , R_o) at RHIC [2, 3, 4]. It does, however, yield the correct normalized oscillation amplitudes for R_s and R_o [5, 6, 7]. We use it here to predict the expected trends for the evolution of the HBT radii at mid-rapidity in ($A\approx 200$) + ($A\approx 200$) collisions from RHIC to LHC, including their normalized oscillation amplitudes in non-central collisions. These trends may be trustworthy, in spite of the model's failure to correctly predict the HBT radii at RHIC.

2. RHIC \rightarrow LHC

Extending the hydrodynamic code AZHYDRO [8] from RHIC conditions to the LHC regime requires a recalculation of the Glauber initial conditions to reflect the achieved higher initial energy density and temperature. Some of the expected trends were outlined in [9] where the initial temperature was increased to 2 GeV to show the possibility of a transition from out-of-plane to in-plane deformation of the freeze-out source in non-central Pb+Pb collisions. Such extreme initial temperatures are, however, not likely to be reached in Pb+Pb collisions at the LHC. We here present predictions for a more realistic range of initial conditions and a better equation of state (EoS) than the ideal quark-gluon gas without phase transition used in [9].

Hydrodynamics cannot predict its own initial conditions as a function of \sqrt{s} , but it does provide a unique relation between the initial entropy density profile and the final hadron multiplicity. The predicted increase of the final charged multiplicity from various models ranges from less than twice to more than 4 times the multiplicity at RHIC [10, 11]. We therefore present our results as a function of final charged multiplicity, parameterizing it through the initial peak entropy density s_0 at thermalization time τ_0 in $b=0$ collisions. We cover the range from $\frac{dN_{ch}}{dy}(y=b=0) = 680$ (RHIC) to $\frac{dN_{ch}}{dy}(y=b=0) = 2040$ (LHC).

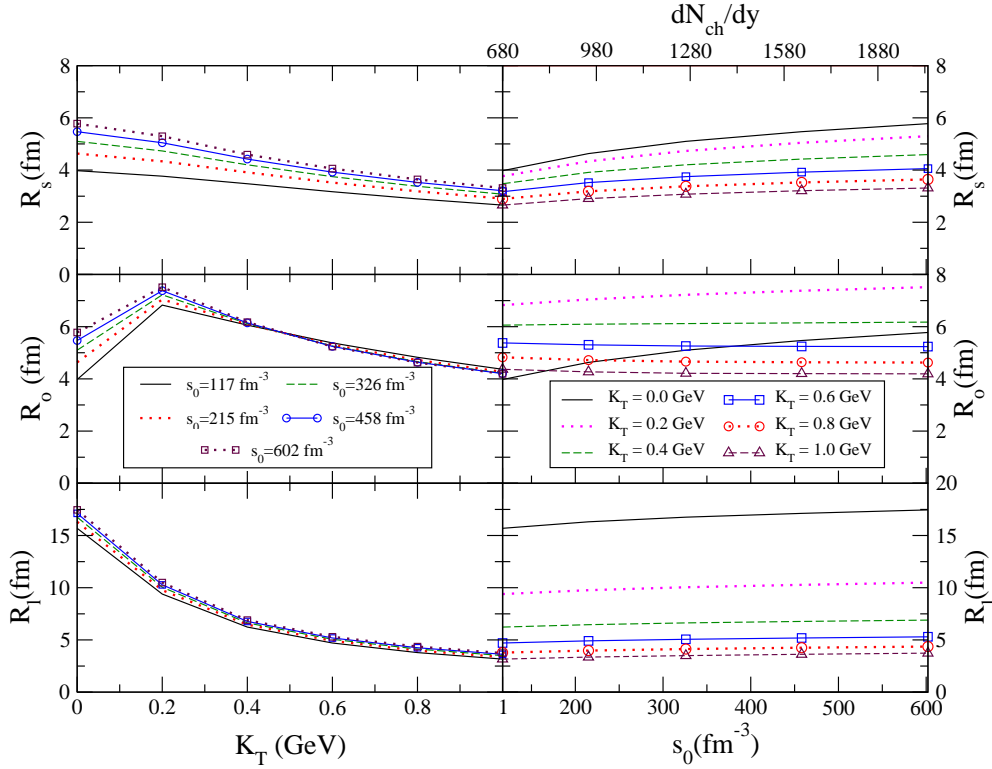


Figure 1. (Color online) Pion HBT radii for central ($b=0$) Au+Au collisions as a function of transverse pair momentum K_T (left) and of initial entropy density s_0 or final charged multiplicity $\frac{dN_{ch}}{dy}$ (right).

We use an EoS that transitions from an ideal quark-gluon plasma phase above a critical temperature T_c to a chemically non-equilibrated hadron resonance gas below T_c (RappEoS [8]). The final hadron yields are assumed to freeze out directly at $T_c = 164$ MeV. The hadron momenta are taken to decouple at energy density $\epsilon_{dec} = 0.075$ GeV/fm³, $T_{dec} = 100$ MeV. Spectra and HBT radii are calculated from the emission function obtained via the Cooper-Frye prescription [12] along this decoupling surface. For simplicity, we compute the HBT radii from the space-time variances of this emission function instead of doing a Gaussian fit to the two-pion correlation function, knowing that this overestimates the longitudinal radius R_l by 20-25% [4]. A corresponding overall downward correction should thus be applied to all R_l values shown below.

As the initial entropy density s_0 and temperature T_0 increase we reduce the thermalization time τ_0 , keeping $T_0\tau_0$ constant. This yields a reduction from $\tau_0 = 0.6$ fm/c for $s_0 = 117$ fm⁻³, $\frac{dN_{ch}}{dy} = 680$ (“RHIC initial conditions”) to $\tau_0 = 0.35$ fm/c for $s_0 = 602$ fm⁻³, $\frac{dN_{ch}}{dy} = 2040$ (“LHC initial conditions”).

3. Central collisions

Figure 1 shows the pion HBT radii for central Au+Au (Pb+Pb) collisions in the out-side-long coordinate system [7] as functions of transverse momentum and total

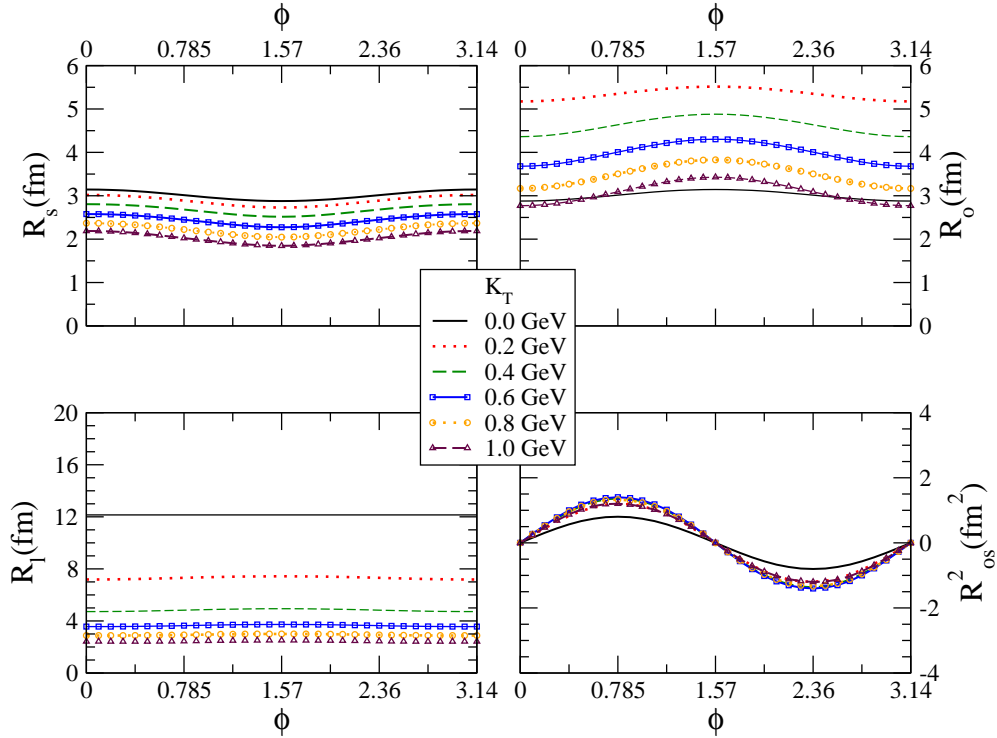


Figure 2. (Color online) Pion HBT radii for non-central ($b=7$ fm) Au+Au collisions as a function of azimuthal angle Φ for different pair momenta K_T , for “RHIC” initial conditions (see text).

charged multiplicity. There are no dramatic changes, neither in magnitude nor in K_T -dependence, of the HBT radii as we increase the charged multiplicity by up to a factor 3. The largest increase is seen for R_s (by $\sim 30\%$ at low K_T) while R_o (which follows R_s at $K_T=0$ by symmetry) even slightly decreases at large K_T . R_l changes hardly at all. For comparison we also performed calculations with a transitionless ideal massless gas EoS [9] (not shown graphically). In this case we see the smallest ($< 10\%$) increase in R_s , about 10-15% increase in R_o (at all K_T), and about 25-30% increase in R_l . None of these changes will be easy to measure, but one sees that differences in the small predicted changes depend on the EoS, in particular on whether or not it embodies a phase transition. The main deficiency of hydrodynamic predictions for the HBT radii at RHIC (too weak K_T -dependence of R_s and R_o and a ratio R_o/R_s much larger than 1) is not likely to be resolved at the LHC unless future LHC data completely break with the systematic tendencies observed so far [3].

4. Non-central collisions

One of the strengths of AZHYDRO is simulating anisotropic, non-central collisions. For RHIC initial conditions, although the magnitudes of the HBT radii in central collisions were not predicted accurately, their normalized oscillation amplitudes at small K_T (which measure the source eccentricity at freeze-out [5]) were correctly

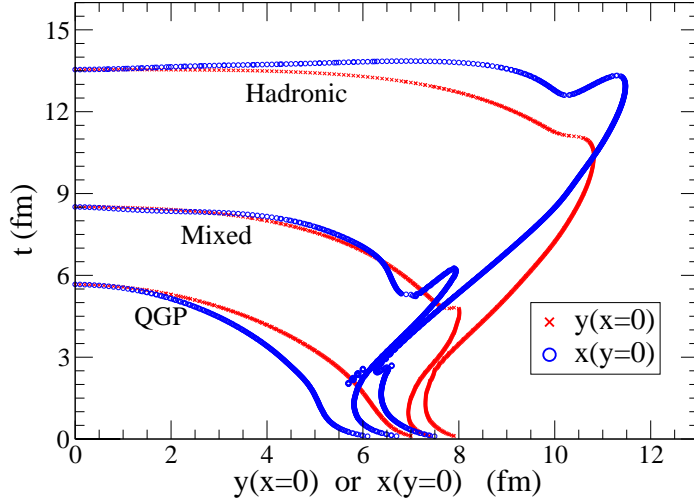


Figure 3. (Color online) Cuts along the x and y axes through the freeze-out surface for (modified) “LHC” initial conditions: $\frac{dN_{ch}}{dy} = 2035$, $s_0 = 1735 \text{ fm}^{-3}$ at $\tau_0 = 0.1 \text{ fm}/c$ (this particular calculation was done for computation of photons and dileptons, using a reduced thermalization time to also capture some of the pre-equilibrium radiation).

reproduced [7]. Their extrapolation to LHC initial conditions may therefore have predictive power.

In Figures 2 and 4 we show the azimuthal oscillations of the HBT radii for semiperipheral Au+Au collisions at $b=7 \text{ fm}$, for both “RHIC” and “LHC” initial conditions defined above. At low pair momentum K_T , both R_s and R_o show an inversion of the sign of the oscillation amplitude between RHIC and LHC. This is indicative of a transition from out-of-plane to in-plane deformation of the source at freeze-out [9]. Figure 3 shows cuts through the decoupling surface (as well as through the hypersurfaces indicating the transition from QGP to mixed phase and from mixed phase to hadron gas) along the x and y axes (in-plane and out-of-plane, respectively) for “LHC” initial conditions: one observes that the source is initially wider in the y -direction (out-of-plane), but later becomes larger in the x -direction (in-plane). With an ideal gas EoS this shape transition requires much higher initial entropy densities and temperatures [9].

Retiere and Lisa [5] introduced the normalized 2nd order Fourier components

$$\frac{R_{(o,s),2}^2}{R_{s,0}^2} = \frac{R_{(o,s)}^2(0) - R_{(o,s)}^2(\frac{\pi}{2})}{R_s^2(0) + R_s^2(\frac{\pi}{2})}, \quad (1)$$

$$\frac{R_{(os),2}^2}{R_{s,0}^2} = \frac{R_{(os)}^2(\frac{\pi}{4}) - R_{(os)}^2(\frac{3\pi}{4})}{R_s^2(0) + R_s^2(\frac{\pi}{2})}, \quad \frac{R_{l,2}^2}{R_{l,0}^2} = \frac{R_l^2(0) - R_l^2(\frac{\pi}{2})}{R_l^2(0) + R_l^2(\frac{\pi}{2})}$$

of $R_{o,s,l}^2(\Phi)$, shown in Figure 5 as functions of K_T and s_0 . They showed [5] that the zero-momentum limit of $R_{s,2}^2/R_{s,0}^2$ is a direct measure of the spatial source eccentricity at freeze-out: $\epsilon_x^{fo} = 2 \lim_{K_T \rightarrow 0} (R_{s,2}^2/R_{s,0}^2)$. Using this relationship, the lower left panel in Figure 5 shows that the freeze-out source eccentricity flips sign between RHIC and LHC, and that at LHC the freeze-out source is elongated in the reaction plane

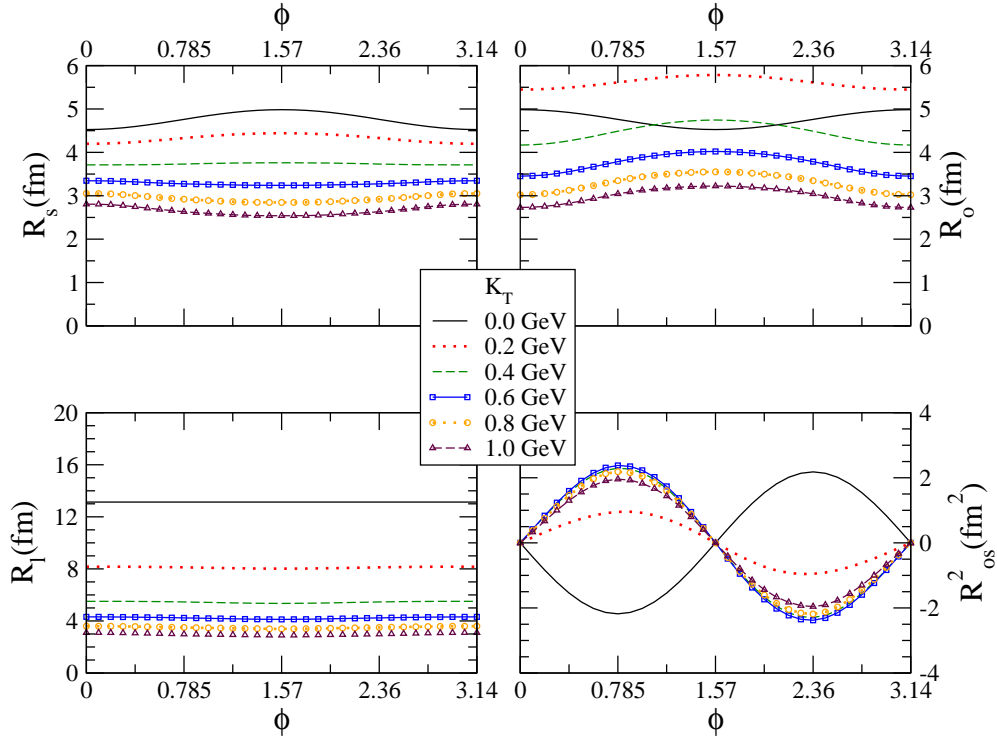


Figure 4. (Color online) Same as Figure 2, but for “LHC” initial conditions.

direction by about as large a factor as it was still out-of-plane elongated in the RHIC case. This is different in runs with an ideal massless gas EoS where even with “LHC initial conditions” the final freeze-out source is found to be still out-of-plane elongated (although just barely so).

5. Conclusions

By varying the initial entropy density to control the final charged multiplicity, we used the hydrodynamic model to predict trends for the pion HBT radii from Au+Au or Pb+Pb collisions as one moves from RHIC to LHC energies. In spite of a documented failure of the hydrodynamic model to reproduce the HBT radii measured at RHIC, the model has had great success for most other soft-hadron observables, so the predicted trends may still be trustworthy. We find very little variation in the HBT radii for central collisions, and whatever small differences we see depends sensitively on details of the equation of state, in particular whether or not it embodies a quark-hadron phase transition. Clear and characteristic changes are predicted for the normalized azimuthal oscillation amplitudes of the HBT radii from non-central collisions, indicative of a qualitative change of the shape of the source at freeze-out which evolves from an out-of-plane elongated freeze-out configuration at RHIC to an in-plane elongated shape at the LHC.

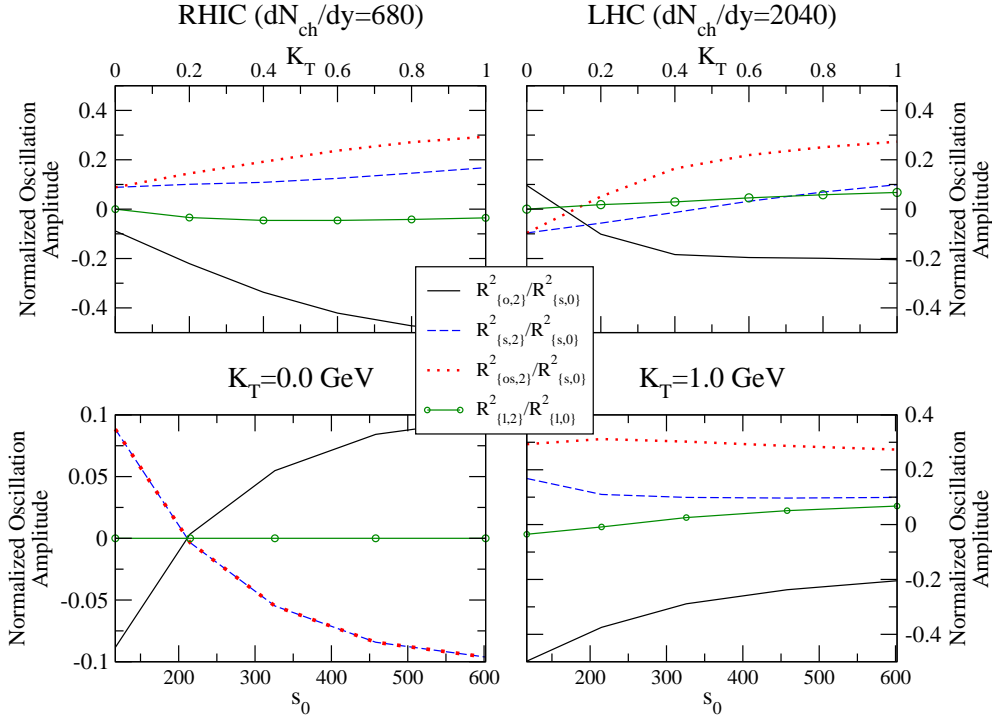


Figure 5. (Color online) Normalized HBT oscillation amplitudes as a function of K_T at RHIC and LHC (top) and as function of s_0 for two values of K_T (bottom).

Acknowledgements: This work was supported by the U.S. Department of Energy under grant DE-FG02-01ER41190 and a University Presidential Fellowship from The Ohio State University (E.F.).

References

- [1] Kolb P F and Heinz U 2003 in: *Quark-Gluon Plasma 3*, edited by R. C. Hwa and X.-N. Wang (Singapore: World Scientific) p. 634
- [2] Heinz U and Kolb P F 2002 in: *Proceedings of the 18th Winter Workshop on Nuclear Dynamics*, edited by R. Bellwied, J. Harris and W. Bauer (Debrecen: EP Systema) p. 205 [arXiv:hep-ph/0204061]
- [3] Lisa M A, Pratt S, Soltz R and Wiedemann U 2005 *Ann. Rev. Nucl. Part. Sci.* **55** 357
- [4] Frodermann E, Heinz U and Lisa M A 2006 *Phys. Rev. C* **73** 044908
- [5] Retiere F and Lisa M A 2004 *Phys. Rev. C* **70** 044907
- [6] Adams J *et al* (STAR Collaboration) 2003 *Phys. Rev. Lett.* **92** 062301
- [7] Heinz U 2006 *Concepts of heavy ion physics*, in *2003 CERN-CLAF School of High-Energy Physics*, edited by N. Ellis, CERN Yellow Report CERN-2006-001, p.165 [arXiv:hep-ph/0407360]
- [8] Kolb P F, Sollfrank J and Heinz U 2000 *Phys. Rev. C* **62** 054909;
Kolb P F and Rapp R 2002 *Phys. Rev. C* **67** 044903;
the code can be downloaded from <http://nt3.phys.columbia.edu/people/molnard/OSCAR/>
- [9] Heinz U and Kolb P F 2002 *Phys. Lett. B* **542** 216
- [10] Kharzeev D, Levin E, and Nardi M 2005 *Nucl. Phys. A* **747** 609
- [11] See contributions by Busza, Bass, Capella, Eskola, Milhano, Kharzeev, Ko, Porteboeuf, Ranft, Salgado, Topor Pop, and Werner in this volume
- [12] Cooper F and Frye G 1974 *Phys. Rev. D* **10** 186